# Modifying the surface energy and hydrophobicity of the low-density silica aerogels through the use of combinations of surface-modification agents

**A. Parvathy Rao · A. Venkateswara Rao**

**Abstract** Aerogels are lightweight, highly transparent, thermally insulating materials comprising interconnected nanostructured pores. Low surface energy aerogels were prepared from ambient pressure drying of sodium silicate-based gels by modifying the pore surfaces with silylating agents including trimethylchlorosilane (TMCS), hexamethyldisiloxane (HMDSO), and hexamethyldisilazane (HMDZ), in combination with each other. Hydrophobic properties of the resulted aerogels were studied by contact angle measurements. Fourier-transform infrared spectroscopy (FTIR) was used to monitor the changes in chemical bonds within the aerogels due to surface modification. The microstructure was studied by transmission electron microscopy (TEM). Effect of temperature on the hydrophobicity of the aerogels was studied by thermogravimetric analysis/differential thermal analysis (TGA-DTA). Surface modification of silica gels with various mixtures of surface-modification agents showed different behaviors. Aerogels made by HMDZ and HMDSO combination comprised 5 nm pores and particles and showed a high surface energy, whereas aerogels prepared by HMDSO and TMCS combination had lower surface energy with relatively larger particle and pore sizes with a more uniform distribution of both. The properties of the latter sample were attributed to a greater degree of surface modification and negligible condensation of OH groups. This preparation produced silica aerogels with a low density (0.042 g/cc), low surface energy (3.39 N cm$^{-1}$), low thermal conductivity (0.050 W K$^{-1}$ m$^{-1}$), high optical transmission (85% at 700 nm) and hydrophobic (154° contact angle) with high hydrophobic

thermal stability (425 °C). Moreover, the contact angle for materials prepared by this method decreased negligibly over 12 months' storage in ambient conditions.

## Introduction

The unique properties of aerogels such as extreme low density ($\sim$0.030 g/cm$^3$), high porosity (>98%), low thermal conductivity ($\sim$0.04 W/mK), low refractive index ($\sim$1.01–1.1), high surface area ($\sim$1000 m$^2$/g), low dielectric constant (<2), optical transparency (95%) and low sound velocity (100 m/s), make the aerogels potentially attractive as excellent transparent thermal insulation materials for double glazed windows [1, 2] and materials for acoustic barriers and catalytic supports [3], absorption of oils [4, 5], and aerosol collectors [6, 7]. Aerogels are sol–gel-derived materials, first prepared by Kistler [8] in 1931 by exchanging the water with the solvent followed by removal of trapped solvents from wet gel by supercritical drying while maintaining the integrity and high porosity of the gel. This method is a dangerous, costly, and involved in high temperatures, pressures, and highly flammable solvents. And also the aerogels were hydrophilic as they have OH end groups and the structure of the aerogels collapsed in the humid atmosphere with time. To nullify these draw backs, an ambient pressure drying method was used for the preparation of the aerogels, in which the hydrophilicity as well as collapse of the gels by condensation of surface OH groups, causing the shrinkage of the gels, was over come by surface modification of the gels with alkyl end group agents to replace the H of the OH with Si–CH$_3$. Surfaces with a water contact angle above 150° (super hydrophobic surfaces) have recently been attracting a great deal of attention because of its small contact area with water,

A. Parvathy Rao (✉) · A. Venkateswara Rao
Air Glass Laboratory, Department of Physics, Shivaji University, Kolhapur, Maharashtra 416 004, India
e-mail: parvathyshivaj@gmail.com

chemical, and bonding formation through water are limited. Therefore, various phenomena such as adherence of rain drops, oxidation, and friction drag are expected to be inhibited on such surface [9].

Ambient pressure drying is a method developed for the preparation of the aerogels from surface modified gel to annihilate the capillary pressure of a wet gel whose pores contain a solvent, rise to capillary pressure, $P_c$, which causes irreversible shrinkage and, eventually cracking of the gel [10, 11]

$$P_c = -\gamma_{lv} \times \cos\theta / r_{pore} \tag{1}$$

$\gamma_{lv}$ is the liquid–vapor surface tension, $\theta$, is the contact angle between the liquid and pore wall, and $r_{pore}$ is the pore radius. To reduce the capillary pressure in the gel network, the surface modification of the pore wall of a wet $SiO_2$ gel from hydrophilic to hydrophobic using the silylating agents carrying hydrophobic functional groups, which reacts with OH groups, is essential. Silylating agents reduces the density of OH groups on the $SiO_2$ surface thereby preventing the $\equiv Si-O-Si \equiv$ bonds, which otherwise might eventually initiate significant shrinkage of the aerogel [12–18]. In other words, as the surface of the aerogel becomes hydrophobic, the extent of moisture adsorption on the silica surfaces and thus the surface tension force arising from the leaving of the solvent from the wet gel would decrease significantly, and the possibility of obtaining monolithic aerogels is increased. Many agents are available for surface-modification process, such as methyltrimethoxysilane (MTMS), dimethyldimethoxysilane (DMDS), trimethyl chlorosilane (TMCS), hexamethyldisiloxane (HMDSO), hexamethyldisilazane (HMDZ), etc.

The aerogels are essentially a special kind of materials which has a large solid–vapor interface area. Owing to their unusual microstructure, aerogels are extremely sensitive to even slight change in surface energy. The present paper deals with the study of the effect of the various combinations of surface-modification agents (CSMAs) such as HMDSO, HMDZ, and TMCS for surface modification for the preparation of low surface energy and highly hydrophobic aerogels along with low density and low thermal conductivity using sodium silicate precursor.

## Experimental

Silica hydrogels were prepared by single step sol–gel process by hydrolysis and polycondensation of sodium silicate precursor in the presence of an ammonium hydroxide catalyst. Surface modification has been done with the combination of HMDSO + HMDZ (A), HMDZ + TMCS (B) and HMDSO + TMCS (C). The chemicals were sodium silicate [($Na_2SiO_3$), LOBA, India, of 1.39 specific gravity

with $Na_2O{:}SiO_2$ weight ratio of 1:3.33] and ammonium hydroxide, Merck, India, methanol, hexane from Sd. fine chemicals, India and silylating agents, HMDSO, TMCS, and HMDZ from Sigma Aldrich Chemie, puram grade of >98%, Switzerland. Triple distilled water was used for the preparation of the solutions. Systematic preparation of the samples contains following steps and also shown in Fig. 1.

### Preparation of the silica wet gel

Silica hydrosols were prepared from the silicic acid which was resulted by passing the 1.10 specific gravity sodium silicate solution obtained from the dilution of original solution, through Amberlite 120 $Na^+$ cation resin and addition of 0.1 mL 1 M ammonium hydroxide to the 25 mL of silicic acid. The sol was poured into 150 mL bottles of 5 cm diameter. Gels were formed in 10 min at room temperature and the strength of the wet gels might be performed by aging the gels subsequently to gelation by putting the gels for 3 hours at 50 °C in the oven followed by placing the gels in water for 24 h at 50 °C.

### Washing of the silica wet gel

The wet gel which contains water in the pores was exchanged with methanol for 24 h at 50 °C to get alcogel. The exchange of water with methanol is needed before the surface modification of the gel with silylating agents, as silylating agents violently react with water.
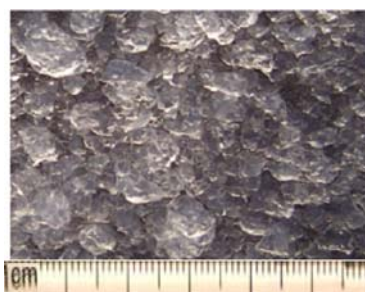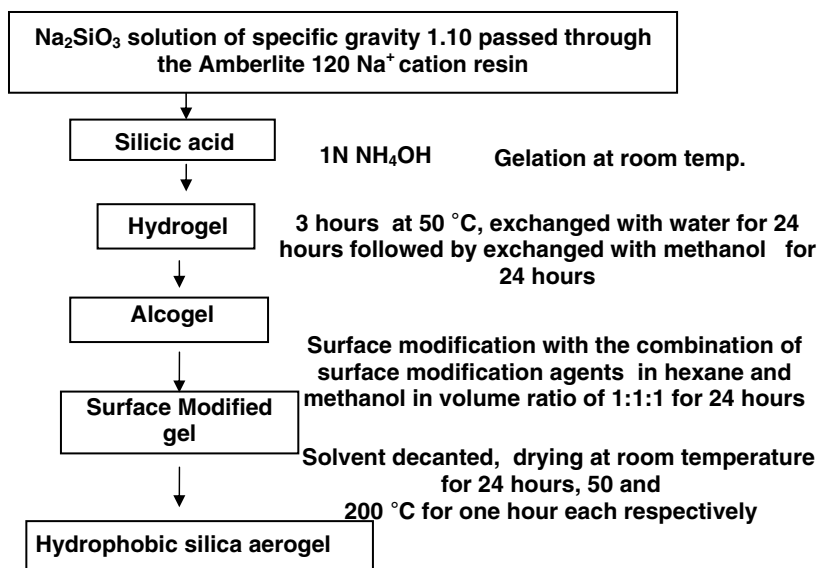
### Surface modification of the alcogels

The surface modification of the alcogels is necessary in the process of ambient pressure drying aerogels because due to presence of surface organic end groups, the capillary pressure arises during the drying of the wet gel become negligible and leads to low density aerogels. Surface modification was carried out with the various CSMAs of A, B, and C in the presence of hexane and methanol with the volume ratio of the hexane, methanol, and CSMA mixture was 1:1:1. The alcogels were immersed in the silylating mixture for 24 h at 50 °C. Due to surface modification, the surface characteristics of the wet gel was changed from hydrophilic to hydrophobic and resulted gels floated over the solution because of low density.

### Drying of the modified gel

Solvent mixture was decanted and alcogels were kept for drying at room temperature for 24 h to evaporate the solvent from the gel and heated at 50 °C followed by 200 °C for 1 h each in the PID controlled oven with heating rate of 24 °C/hour. The gels were cooled and used for characterization.

**Fig. 1** Preparation of the silica aerogels with photos of the various surface-modification agent mixtures



Na₂SiO₃ solution of specific gravity 1.10 passed through the Amberlite 120 Na⁺ cation resin

→ **Silicic acid**     1N NH₄OH     Gelation at room temp.

→ **Hydrogel**     3 hours at 50 °C, exchanged with water for 24 hours followed by exchanged with methanol for 24 hours

→ **Alcogel**     Surface modification with the combination of surface modification agents in hexane and methanol in volume ratio of 1:1:1 for 24 hours

→ **Surface Modified gel**     Solvent decanted, drying at room temperature for 24 hours, 50 and 200 °C for one hour each respectively

→ **Hydrophobic silica aerogel**

**HMDZ+HMDSO aerogels**          **HMDZ+TMCS aerogels**

**HMDSO+TMCS aerogels**

Sample characterization

*Density and porosity*

Apparent density of the aerogels was obtained by using the weight with microbalance of $10^{-5}$ g accuracy and volume of the aerogels.

The volume shrinkage was obtained from the

$$\% \text{ of volume shrinkage} = \left(1 - V_a/V_g\right) \times 100 \qquad (2)$$

where $V_g$ and $V_a$ are the volumes of the wet gel and aerogel, respectively.

The % of porosity and pore volume were calculated using the following equations:

$$\% \text{ of porosity} = (1 - \rho_b/\rho_s) \times 100 \qquad (3)$$

$$\text{Pore volume} = (1/\rho_b - 1/\rho_s)\text{cc/g} \qquad (4)$$

where $\rho_b$ and $\rho_s$ are the bulk density and skeletal density (1.98 g/cc) of the silica aerogels, respectively.

*Thermal conductivity*

Thermal conductivity, K, of the aerogels was determined with ring probe method, by putting the similar samples

above and below the ring in thermal conductivity meter [C-T meter from Teleph Company, France]. Before measurements, the instrument was calibrated with a standard sample of 0.035 W/m K thermal conductivity.

### Contact angle measurement

Static contact angle, advancing and receding angles of silica aerogel were measured from a water drop of 0.5 mm diameter placed on the sample surface using rame' hart contact angle meter, USA.

### Fourier transform infrared (FTIR)

Fourier Transform Infrared (FTIR) spectroscopic studies of the aerogels were carried out for various chemical bonds such as –OH, Si–OH, C–H, Si–C and Si–O–Si using Perkin Elmer (Model no. 760 × in 400–4000 cm$^{-1}$ range) IR spectrophotometer. Aerogel pieces were ground with the KBr and processed to form a sample disk in form of pellet for FTIR measurements.

### BET analysis

The surface area, pore volume, and mean pore size of the samples were obtained from the BET analyses (pore size 0.35–200 nm, 0.01 m$^2$/g). Pore size distributions were measured via BJH desorption cumulative pore volume method. Before N$_2$ adsorption, the samples were degassed at 200 °C.

### TEM micrographs

TEM micrographs of the aerogels have been taken with Transmission Electron Micrometer, (Philips, Tecnai, F20 model, The Netherlands) in the range of 50 to 100 nm to find the microstructure of the aerogels.

### TGA-DTA

Thermal stability of the aerogels has been studied from thermo gravimetric and differential thermal analysis (TGA-DTA) to find retention of hydrophobicity with temperature in the temperature range from room temperature to 600 °C with TGA-DTA, SDT, 2960TA meter, USA.
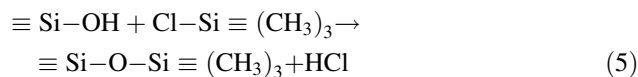
## Results and discussion

Generally, TMCS was widely used for the surface modification of the wet gel to produce the aerogels by ambient pressure drying method with Tetraethylorthosilciate
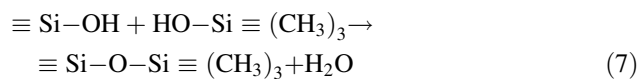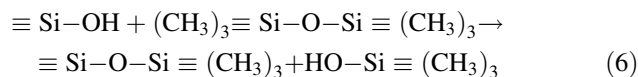
(TEOS) and sodium silicate precursors [19, 20]. But there are some draw backs arising with the TMCS as it is highly reactive surface modifying agent produced opaque aerogels. To overcome this problem surface modification of the silica surface was carried out using various CSMAs such as A, B, and C.

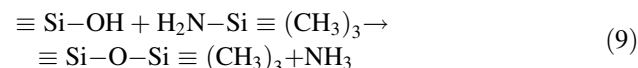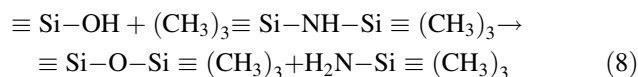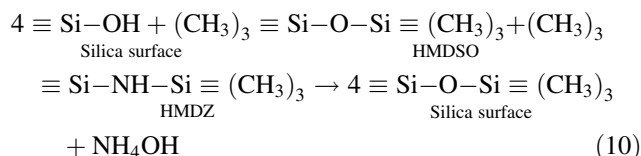Reactions of TMCS, HMDSO, and HMDZ with silica surface:

With TMCS

$$\equiv \text{Si}-\text{OH} + \text{Cl}-\text{Si} \equiv (\text{CH}_3)_3 \rightarrow$$
$$\equiv \text{Si}-\text{O}-\text{Si} \equiv (\text{CH}_3)_3 + \text{HCl} \tag{5}$$

With HMDSO

$$\equiv \text{Si}-\text{OH} + (\text{CH}_3)_3 \equiv \text{Si}-\text{O}-\text{Si} \equiv (\text{CH}_3)_3 \rightarrow$$
$$\equiv \text{Si}-\text{O}-\text{Si} \equiv (\text{CH}_3)_3 + \text{HO}-\text{Si} \equiv (\text{CH}_3)_3 \tag{6}$$

$$\equiv \text{Si}-\text{OH} + \text{HO}-\text{Si} \equiv (\text{CH}_3)_3 \rightarrow$$
$$\equiv \text{Si}-\text{O}-\text{Si} \equiv (\text{CH}_3)_3 + \text{H}_2\text{O} \tag{7}$$

With HMDZ

$$\equiv \text{Si}-\text{OH} + (\text{CH}_3)_3 \equiv \text{Si}-\text{NH}-\text{Si} \equiv (\text{CH}_3)_3 \rightarrow$$
$$\equiv \text{Si}-\text{O}-\text{Si} \equiv (\text{CH}_3)_3 + \text{H}_2\text{N}-\text{Si} \equiv (\text{CH}_3)_3 \tag{8}$$

$$\equiv \text{Si}-\text{OH} + \text{H}_2\text{N}-\text{Si} \equiv (\text{CH}_3)_3 \rightarrow$$
$$\equiv \text{Si}-\text{O}-\text{Si} \equiv (\text{CH}_3)_3 + \text{NH}_3 \tag{9}$$

The reactions of A, B, and C with silica surface:

With HMDSO + HMDZ

$$4 \equiv \underset{\text{Silica surface}}{\text{Si}-\text{OH}} + \underset{\text{HMDSO}}{(\text{CH}_3)_3 \equiv \text{Si}-\text{O}-\text{Si} \equiv (\text{CH}_3)_3} + (\text{CH}_3)_3$$
$$\equiv \underset{\text{HMDZ}}{\text{Si}-\text{NH}-\text{Si} \equiv (\text{CH}_3)_3} \rightarrow 4 \equiv \underset{\text{Silica surface}}{\text{Si}-\text{O}-\text{Si} \equiv (\text{CH}_3)_3}$$
$$+ \text{NH}_4\text{OH} \tag{10}$$

With HMDZ + TMCS

$$3 \equiv \underset{\text{Silica surface}}{\text{Si}-\text{OH}} + \underset{\text{HMDSO}}{(\text{CH}_3)_3 \equiv \text{Si}-\text{NH}-\text{Si} \equiv (\text{CH}_3)_3}$$
$$+ \underset{\text{TMCS}}{(\text{CH}_3)_3 \equiv \text{Si}-\text{Cl}} \rightarrow 3 \equiv \underset{\text{Silica surface}}{\text{Si}-\text{O}-\text{Si} \equiv (\text{CH}_3)_3} + \text{NH}_4\text{Cl} \tag{11}$$

With HMDSO + TMCS

$$3 \equiv \underset{\text{Silica surface}}{\text{Si}-\text{OH}} + \underset{\text{HMDSO}}{(\text{CH}_3)_3 \equiv \text{Si}-\text{O}-\text{Si} \equiv (\text{CH}_3)_3}$$
$$+ \underset{\text{TMCS}}{(\text{CH}_3)_3 \equiv \text{Si}-\text{Cl}} \rightarrow 3 \equiv \underset{\text{Silica surface}}{\text{Si}-\text{O}-\text{Si} \equiv (\text{CH}_3)_3} + \text{H}_2\text{O} + \text{HCl} \tag{12}$$

$$(CH_3)_3 \equiv Si-O-Si \equiv (CH_3)_3 + 2HCl \rightarrow$$
$$\underset{HMDSO}{}$$
$$\underset{TMCS}{2Cl-Si \equiv (CH_3)_3 + H_2O} \qquad (13)$$
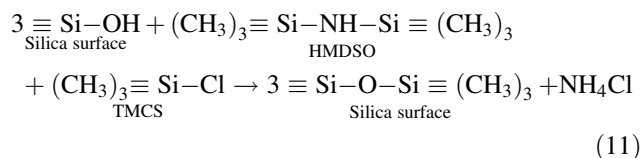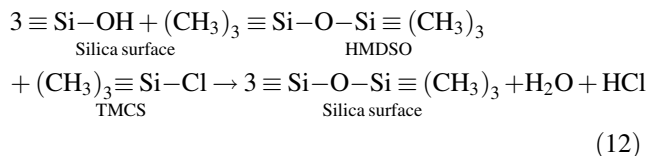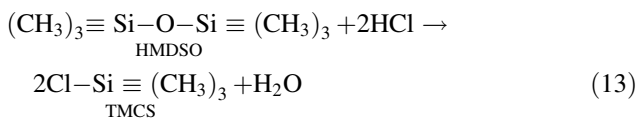
It was reported that by using only TMCS [20], for surface modification of the silica gel, the reaction of TMCS with the gel is very fast with release of HCl as shown in reaction 5, leaving no time for the gel to arrange in a proper and uniform manner to get aerogels with required properties and with HMDSO, surface modification is slow, as it has to under go double dissociation for its two Si–(CH_3)_3 groups to participate in the silylation as shown in Eqs. 6 and 7 and H_2O, by product, inhibits the surface modification. Surface modification with HMDZ is also a two-step process with release of ammonia which enhances the cluster formation as shown in Eqs. 8 and 9. Therefore, it is needed to use the combination of silylating agents to reduce their draw backs and enhance the surface modification of the silica gel. For example, with simultaneous use of the TMCS and HMDSO, the TMCS activity slows down and with release of HCl from TMCS, HMDSO activity increased and helps in the production of more TMCS, more Si–(CH_3)_3 groups as shown in Eqs. 12 and 13. Their individual reactivities were complimentary. Chain reactions occurred and enhanced the surface modification resulting in aerogels with uniform structure, lower density, greater transparency, and hydrophobicity which are unattainable with the use of single silylating agent.

The main point of this work is to achieve the maximum and sufficient surface modification of the wet gel by using the various CSMAs, so that surface characteristics of the wet gel become hydrophobic enough to ensure a sufficient reduction in the surface tension force that arises from the drying stage due to the leaving of solvent. Once the surface tension force is reduced, the volume shrinkage would diminish, leading to a lower apparent density, higher porosity, large pore volume, and a more stable structured aerogel with low surface energy.

Contact angle and surface energy measurements

The contact angle of the aerogels for various CSMAs has been shown in Fig. 2 and found that there is a low contact angle of 85° for the aerogel A, and high contact angle of 154° for aerogel C. The surface energy of the aerogels was measured using the advancing and receding angles as shown in the Fig. 3, using the formula [21].

Surface energy, $Y =$

$$\gamma_l(\cos\theta_r - \cos\theta_a)(1 + \cos\theta_a)^2 \big/ (1 + \cos\theta_r)^2$$
$$- (1 + \cos\theta_a)^2 \qquad (14)$$

$\gamma_l =$ surface tension of the liquid, $a$ is the advancing angle, $r$ is the receding angle. The obtained results are given in Table 1. According to the Young's equation [22, 23], the surface energy relation at equilibrium point of liquid, vapour, and solid is:

$$\gamma_{sl} = \gamma_{sv} - \gamma_{lv}\cos\theta \qquad (15)$$

$\gamma_{sl}$, $\gamma_{sv}$, and $\gamma_{lv}$ are the surface energies of the solid/liquid, solid/vapour, and liquid/vapour phases respectively. It was found from the equation that the surface energy of the



Fig. 2 Water drop over the silica aerogel surface with various surface-modification agent mixtures a HMDSO + HMDZ, b TMCS + HMDZ, and c TMCS + HMDSO
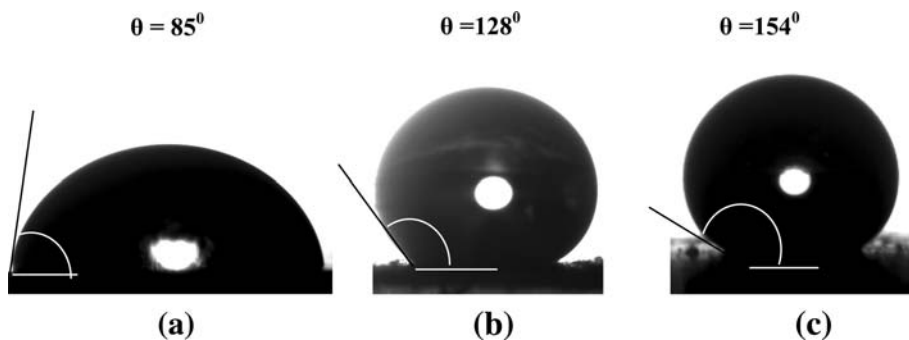
$\theta = 85^0$ (a)    $\theta = 128^0$ (b)    $\theta = 154^0$ (c)



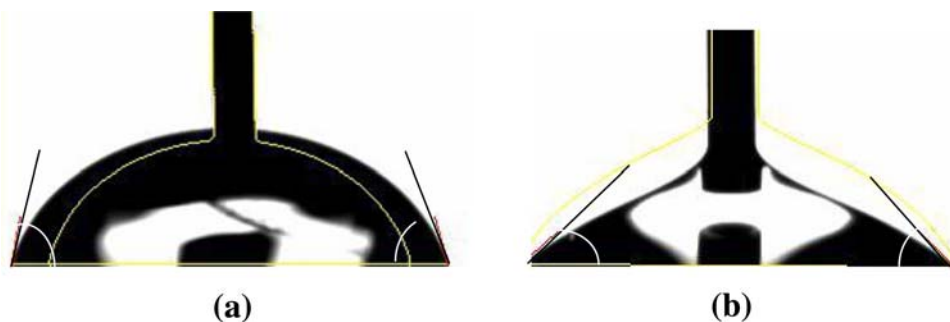Fig. 3 a Advancing and b receding angle

(a)    (b)

**Table 1** Shows the advancing and receding angle and surface energies of the silica aerogels

| Samples | Contact angle (°) | Advancing angle ($a$) | Receding angle ($r$) | Hysteresis ($a - r$) | Surface energy $10^{-5}$ N cm$^{-1}$ |
|---------|-------------------|-----------------------|----------------------|----------------------|--------------------------------------|
| A | 85 | 91 | 79 | 12 | 32.42 |
| B | 128 | 132 | 126 | 8 | 10.81 |
| C | 154 | 156 | 152 | 4 | 3.39 |

solid/liquid interface is less than the sold/vapor interface for the hydrophobic surfaces. Surface energies were calculated from the Eq. 14 for aerogels with various CSMAs and have been shown in the Table 1, and reveals that there is a high surface energy (32.42 N/cm) for the low contact angle (85°) aerogel A, whereas the low surface energy (3.39 N/cm) for high contact angle (154°) aerogel C. It can also be said that low contact angle and high surface energy aerogel A is hydrophilic and the high contact angle and low surface energy aerogel C is hydrophobic. Due to presence of surface OH groups, the high surface energy aerogel A attracts water molecules, making the water drop to spread over the surface and whereas the low surface energy aerogel C with surface organic groups, repels the water drop; hence, water drop encircles the round shape with high contact angle as shown in Fig. 4. Simultaneously, it can also be explained with surface roughness phenomena. There are more OH groups on the surface of the aerogel A

and more O–Si≡(CH₃)₃ groups on the aerogel C surface. Since OH groups are smaller than the branched O–Si≡(CH₃)₃ groups, the surface of the aerogel A is smooth by the smaller OH groups and whereas the surface of the aerogel C is rough by the branched O–Si≡(CH₃)₃ groups as shown in Fig. 4. Surface roughness is one of the testing factors to find the hydrophobicity of the surface; more rough surfaces are more hydrophobic. Hydrophobic properties are enhanced by increasing the surface roughness [24]. Dependence of the wetting characteristics of a solid on the roughness of its surface is inherent and is explained in the fundamental theory of wetting action [25]. Superhydrophobic surface requires both appropriate surface roughness and low surface energy [26]. In the case of hydrophilic surface, due to smooth surface, water drops enter into the surface and spread over it, whereas in the hydrophobic surface, since it has rough surface with organic groups, the water drop does not enter into the

**Fig. 4** Surface roughness of the silica surface **a** Hydrophilic, **b** hydrophobic



(a)                                          (b)
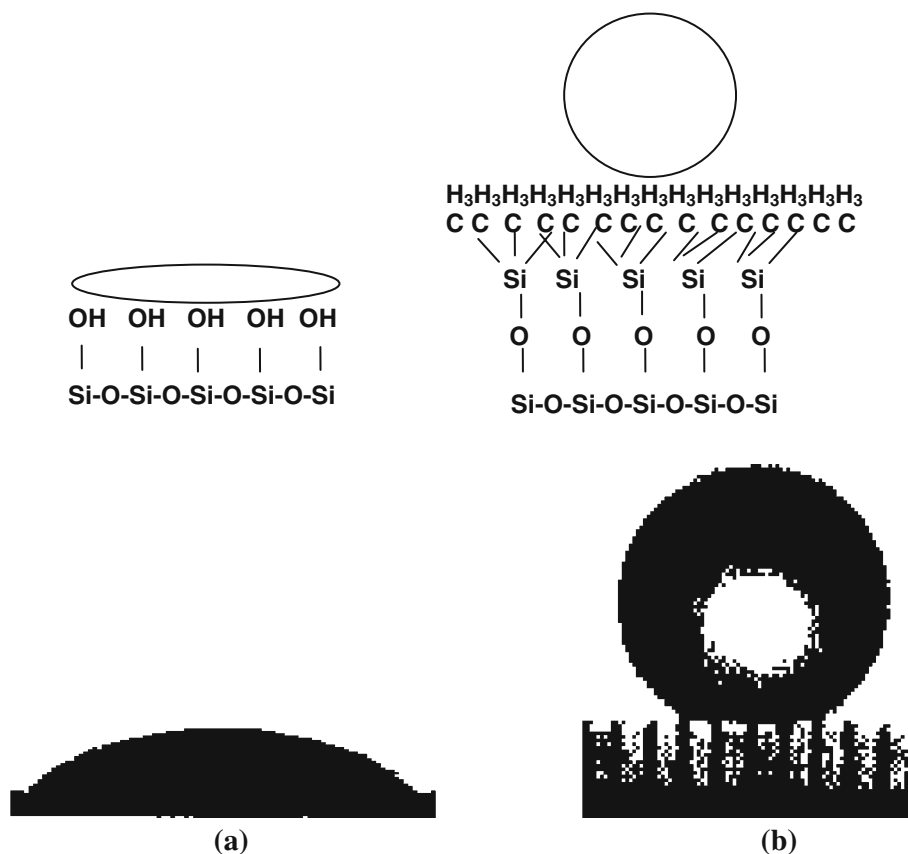
surface as shown in the Fig. 4. Effect of surface roughness versus the contact angle has been extensively discussed in the literature [27, 28]. Very high value of measured contact angle (>150°) has also led to investigate the origins of super-hydrophobicity of the aerogels.

Water repellant surface

Experiments were carried out by moving the aerogel C surface toward a suspended droplet as shown in Fig. 5a, and slowly pushing the sample against the droplet (Fig. 5b). The water droplet suspended over the surface (Fig. 5c). Further, the surface was removed slowly from the water droplet (Fig. 5d) and water droplet started to detach from the surface as shown in Fig. 5e. Subsequently, the sample was removed from the droplet (Fig. 5f). In the process of water drop addition on the hydrophobic surface of aerogel C, the surface was brought toward the water drop which was hanging to needle as shown in the Fig. 5a; when it touched the surface (Fig. 5b), the drop rests over the surface as shown in the Fig. 5c. Due to low surface energy of the hydrophobic surface, it repelled the water drop. The surface energy of the aerogel is lower than the centripetal force of the drop; hence, the water drop encircles round shape with minimum base as shown in the Fig. 5c. It was found that the suspending droplet was difficult to attach to the aerogel surface. Further, the surface was taken away from the drop by bringing the needle toward the water drop as shown in Fig. 5d; as soon as the needle touches water drop, the drop attaches to the needle due to repulsive force of the surface and attractive force of the needle as shown in Fig. 5e. It was found that as soon as the surface was free from the water drop, no visual water

residue was left on the surface of the sample after removing the water droplet as shown in Fig. 5f. After removal of the water drop, the surface characteristics are similar to the surface before addition of the water drop as shown in Fig. 5a, f. This experiment indicated that the adhesion between the droplet and surface of the aerogel is much weaker than that of the needle and the droplet. If the surface has more surface energy, more adhesion, resulting in hydrophilic surface and less surface energy, repulsion of water, resulting in more hydrophobic surface. Structure of the surface of aerogels A is hydrophilic and aerogel C is hydrophobic as shown in Fig. 6.

Some of the physical properties of the aerogels with various CSMAs are shown in Table 2. It was found that the density of the aerogel A is more (0.18 g/cc) and for the aerogel C is low (0.042 g/cc). This is because, the surface modification is less with the A mixture as it is unable to modify all the surface OH groups in the wet gel as shown in Fig. 6, causing more shrinkage during the drying of the gels by condensation of the OH end groups, resulting in dense gels followed by less porosity and low pore volume, less hydrophobic and transparent than the other aerogels as shown in Fig. 1. With C mixture, there is nearly 100% of surface modification in the wet gels as shown in Fig. 6, causing the negligible shrinkage during the drying of the gels resulting in low density, highly porous, and high pore volume aerogels with high hydrophobicity. The aerogels B are opaque as shown in Fig. 1 due to reaction of ammonia from HMDZ and HCl from TMCS forming ammonium chloride precipitation in the gels as shown in Eq. 11, and it retards the surface modification and enhances the cluster formation; therefore, opaque aerogels were obtained and the densities, pore volumes, and % of porosities were in between range of the above said aerogels A and C.

**Fig. 5** Various phases of the water droplet on the hydrophobic aerogel C surface **a** before addition, **b** touching the surface, **c** on the surface, **d** start to remove the surface from the water droplet, **e** detaching the surface, **f** completely surface detached from the water drop let, gaining the water droplet its original shape and also aerogel surface its original one
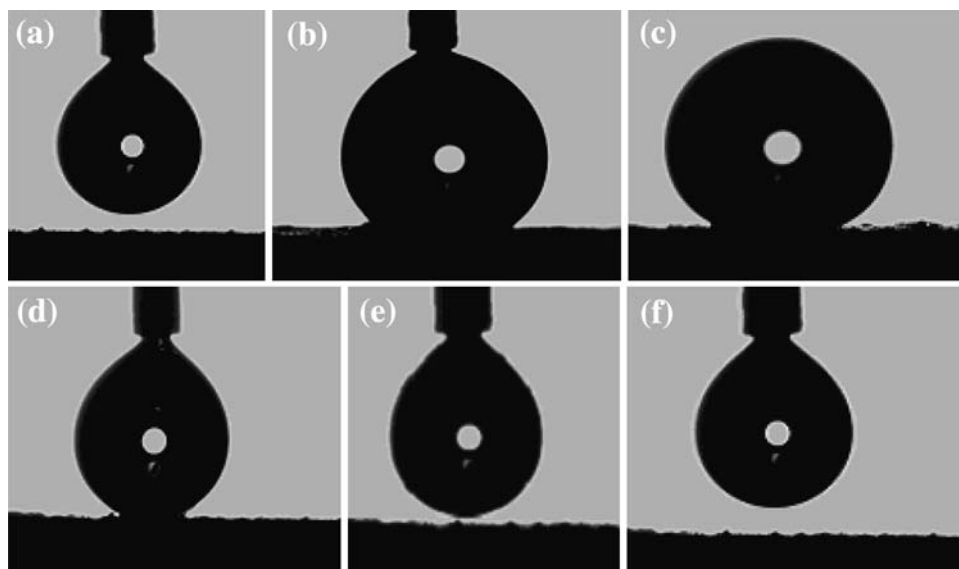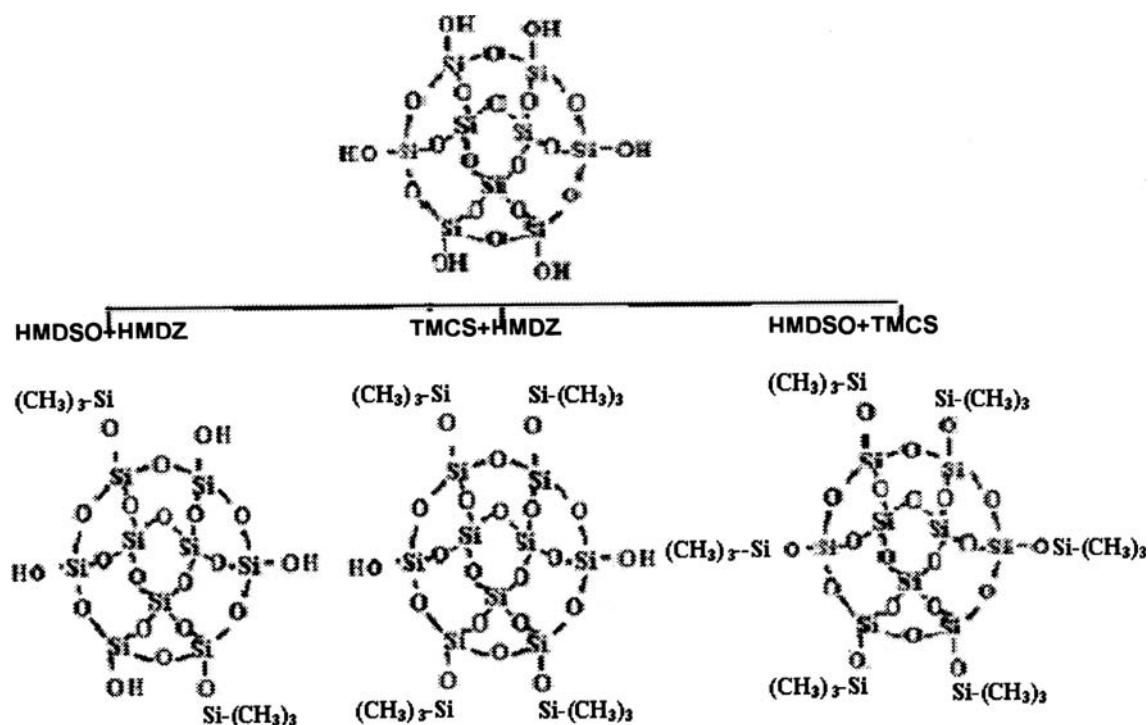
**Fig. 6** Surface modification of the silica gel with various surface-modification agent mixtures

**Table 2** Shows the some of the physical properties of the silica aerogels

| Samples | % of volume shrink age | Density (g/cc) | % Porosity | Pore volume (cc/g) | Thermal conductivity (W/m k) | Surface area (m²/g) | % of optical transmission at 700 nm |
|---------|-----|-----|-----|-----|-----|-----|-----|
| A | 50 | 0.181 | 90.76 | 5.04 | 0.192 | 590 | 95 |
| B | 10 | 0.061 | 96.9 | 16.01 | 0.071 | 495 | 35 |
| C | 3 | 0.042 | 97.85 | 23.33 | 0.050 | 450 | 85 |

## FTIR spectra

To confirm the cause of the surface modification which leads to hydrophobicity, chemically, FTIR has been measured and results have been shown in Fig. 7 for the aerogels with various CSMAs. It was found from the figure that the intensity of the chemical bonds related to OH in the range of 4000 to 2800 cm$^{-1}$, the absorption band near 3500 cm$^{-1}$ stands out and can be attributed to the stretching modes of residual Si–OH and some adsorbed water [29, 30]. In general, this band reflects the amount of residual Si–OH, which is inversely related to the degree of silylation. This band is often accompanied by another at 1600 cm$^{-1}$, which is attributed to the –OH vibrations of molecular water that is physically adsorbed in the network. Because of low intensity of the peak at 1600 cm$^{-1}$, the 3500 cm$^{-1}$ mostly reflects the silanols groups, and whose relative intensities are a good measure of the hydrophilicity of the structure. Evidently, the amount of Si–OH bonding declined significantly with surface modification. In fact in
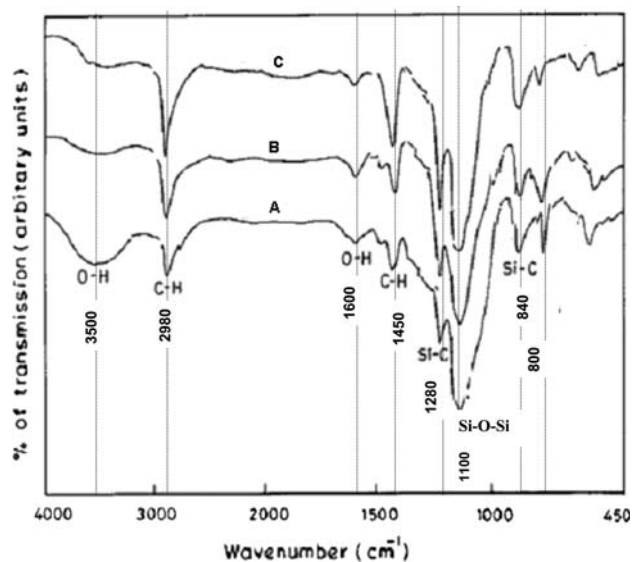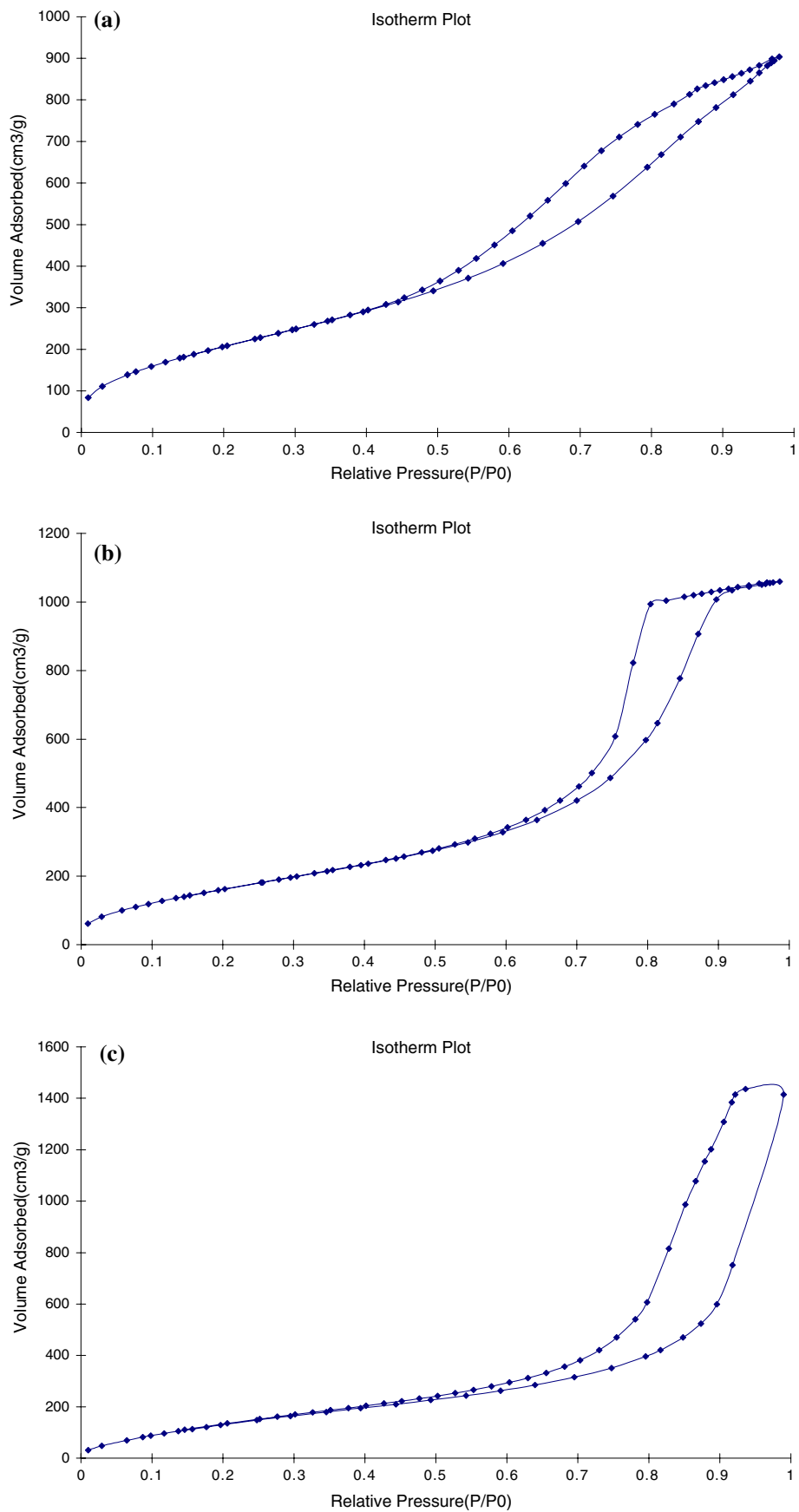


**Fig. 7** FTIR of the aerogels with various surface-modification agent mixtures (A) HMDSO + HMDZ, (B) TMCS + HMDZ, and (C) TMCS + HMDSO

**Fig. 8** N$_2$ adsorption and desorption isotherms of the aerogels with various surface-modification agent mixtures **a** HMDSO + HMDZ, **b** TMCS + HMDZ, and **c** TMCS + HMDSO

the aerogel C, the peak at 3500 cm$^{-1}$ almost disappeared, indicating a rather complete surface modification. Note that the surface modification with C mixture replaced the Si–OH bonding with the Si–O–Si(CH$_3$)$_3$ bonding, thus reducing the signals for Si–OH but yielding peaks located at 2980,1450,1280, and 840 cm$^{-1}$. The intensity of the OH peak is larger and minute (CH$_3$) peaks in the aerogel A [31]. In the mean time, the peak attributed to the adsorbed moisture on the silica surface, manifested as the H–OH bonding and located at 1600 cm$^{-1}$[30] was attenuated drastically with the surface modification and even disappeared for the aerogel C. This is expected, as the tendency of moisture adsorption will be suppressed for more hydrophobic surfaces.

Bands near 2980 and 1450 cm$^{-1}$ as shown in the figure are assigned to C–H stretching and deformation vibrations, and bands at 1280 and 840 cm$^{-1}$ are related to the Si–C bond [32, 33] and are more intense in the aerogel C than the other aerogels. These bonds are responsible for the surface modification by replacing the OH with Si–CH$_3$ resulting in the Si–C and C–H from the Si–CH$_3$ molecule resulting in the more hydrophobic which is also confirmed with contact angle measurements as shown in Fig. 2.

The most intense peak is observed at 1100 cm$^{-1}$ in all aerogel samples due to the asymmetric stretching vibration of the Si–O bond that makes the skeletal SiO$_2$ network [34] and is expected for the silica materials. This band goes together with two bands around 800 and 470 cm$^{-1}$ which are assigned, respectively, to bond bending and bond rocking vibrations of Si–O bonds in the three dimensional SiO$_2$ network. The larger absorbance of bands corresponding to Si–O bonds in aerogel seems to increase the skeletal density and suggests that it enhances the cross linking through condensation of OH groups as shown in Fig. 7A.

## Porous texture

The porous nature of the aerogels has been studied from the N$_2$ adsorption–desorption isotherms of the aerogels with various CSMAs and resulting hysteresis loops of the adsorption/desorption curves for the aerogels have been shown in Fig. 8a–c. According to IUPAC classification, adsorption of the aerogels corresponds to type IV and is characteristic of mesoporous solids [35]. The isotherm type IV with H2 hysteresis loop, associated with the filling and emptying of mesopores through capillary condensation. The nitrogen absorption was linearly increased with the relative pressure until 0.5 and then increased abruptly and saturated at near saturated pressure during absorption process. During desorption, nitrogen was dissociated and the cumulative absorbed volume decreased greatly in the region of 0.65–1 of $P/P_0$. In the mesopore region, in the relative pressure ($P/P_0$) range between 0.30 and 0.90, N$_2$ absorption is more for the aerogel C. Therefore adsorption and desorption branches of the hysteresis loop shifted toward the higher relative pressure. The larger hysteresis loop for the aerogel C indicates more pore volume in the aerogels. For aerogels B and C, the region of great desorption shifted to 0.7–1 and 0.75–1, respectively, than the aerogel A at 0.55–1 and it indicates that the pore size distribution in the aerogels B and C have larger >9 nm than the A aerogel which has small pore size distribution of 5 nm.



Fig. 9 Density, pore volume, and thermal conductivity of the aerogels with various surface-modification agent mixtures (A) HMDSO + HMDZ, (B) TMCS + HMDZ, and (C) TMCS + HMDSO
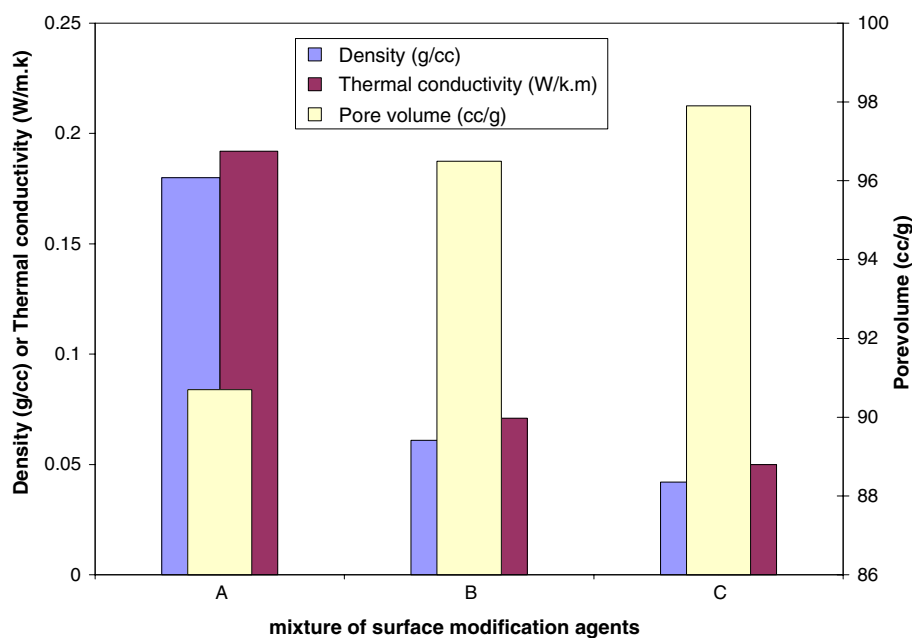
From the $N_2$ adsorption data, it is possible to obtain the textural parameters of the aerogels, so that it can be possible to carry out quantitative comparison of the surface area and pore size values of the aerogels as shown in Table 2. It was found that the surface areas are in the range 500–600 $m^2/g$ for the aerogel A and 400–500 $m^2/g$ for the aerogels B and C. Further characterization on the silica aerogels of FTIR and contact angle measurements have provided solid proof for the success of using mixed agents for surface modification.

Thermal conductivity

Thermal conductivity of the aerogels was measured and has been shown in Fig. 9 and Table 1. The thermal conductivity is low for the aerogels C than the other aerogels. Thermal conductivity is the dependent factor on the density of the aerogels that is silica solid network per unit area. The solid amount per unit area is low for the low density aerogels resulting in low thermal conductivity and highly insulating materials. This is due to the fact that heat flow, which depends on the path in the aerogel network, contains more air along with the solid matrix.

Pore size distribution

Figure 10 shows the pore size distribution of the aerogels measured from nitrogen adsorption method using the Barret–Joyer–Halenda (BJH) method [36] implemented in the software provided with the ASAP2010 adsorption apparatus. From the figure, it was observed that the pore size distribution peak for the aerogel A is sharp and the maxima appears at 5 and at 11 nm for the aerogel C, whereas a broad pore size distribution with the maximum peak was observed at 16 nm for the aerogel B. Aerogels are microporous materials with mesopore volume constituting

over the 92% of the total pore volume, which increases for the aerogels C as shown in Table 1. The aerogel A was highly dense with less surface modified gels and the compliant structure, and can freely shrink in response to solvent removal. The enormous capillary pressure attained



Fig. 11 TEM of the silica aerogels with various surface-modification agent mixtures. **a** HMDSO + HMDZ, **b** TMCS + HMDZ, and **c** TMCS + HMDSO
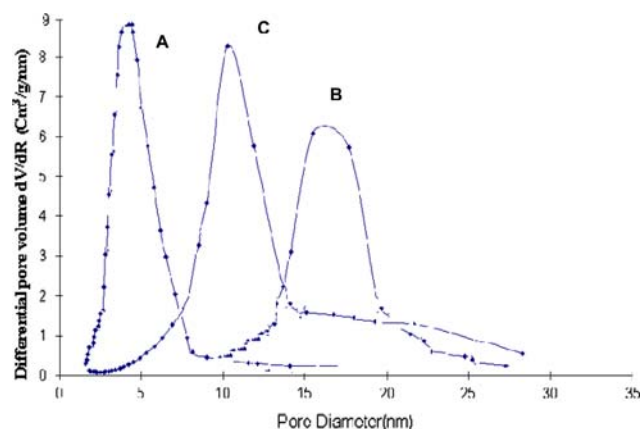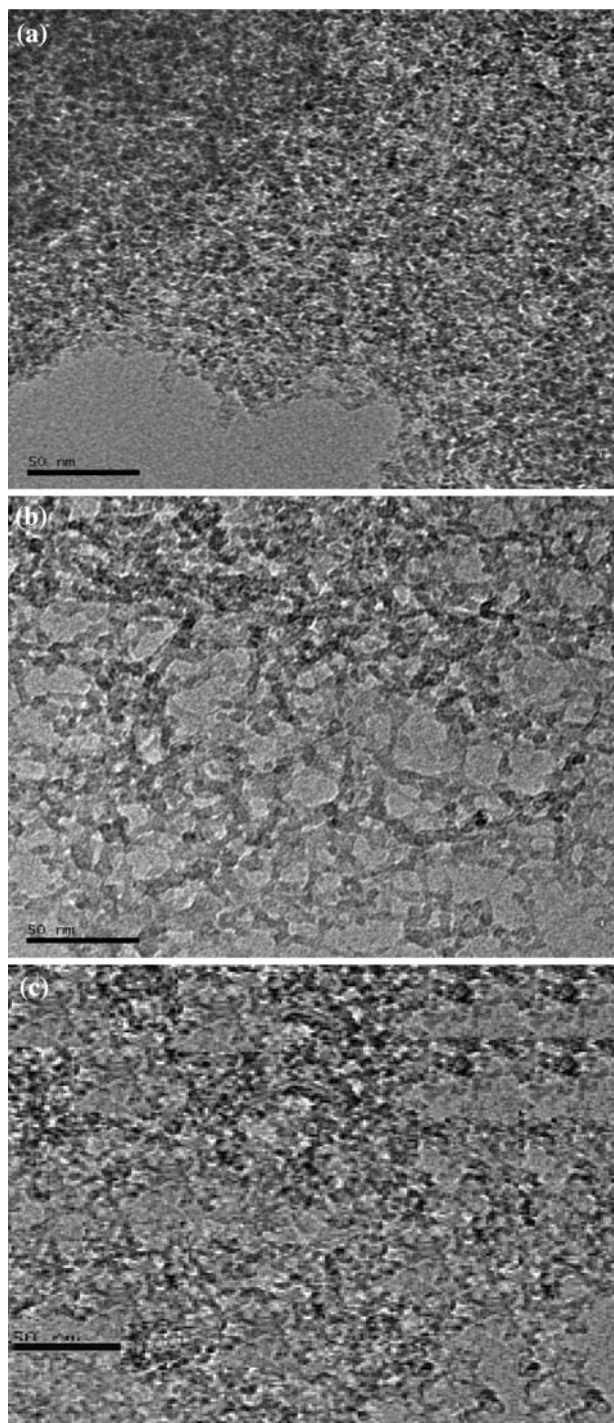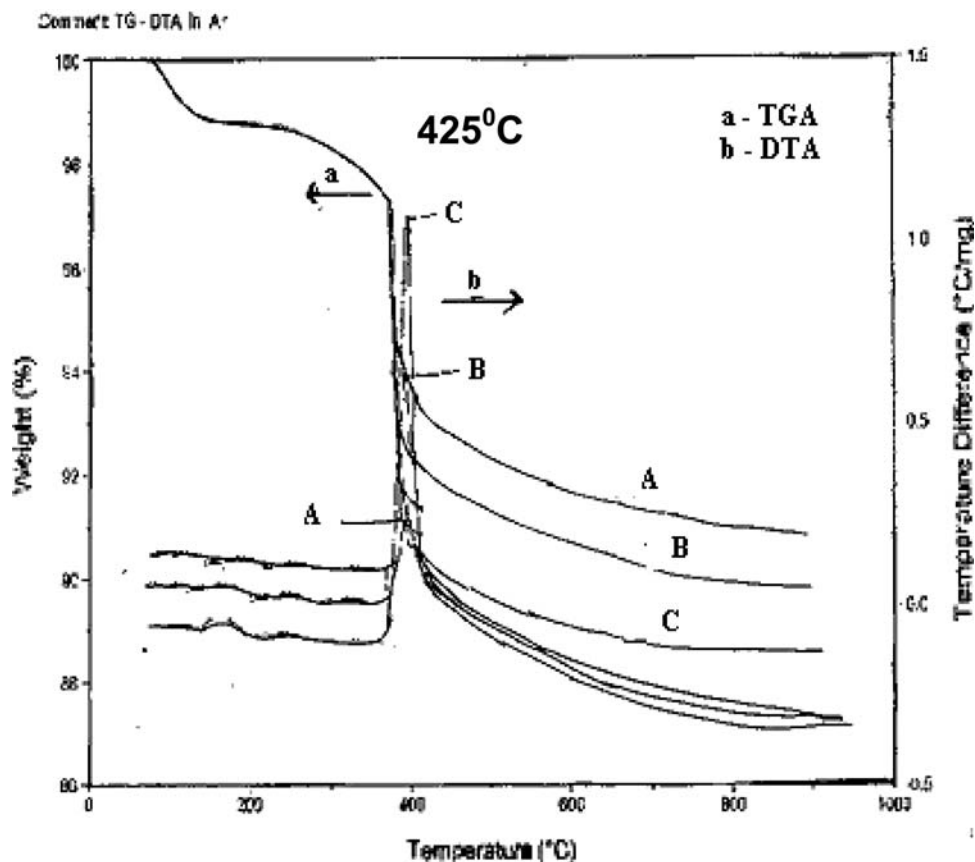


Fig. 10 Pore size distribution in the silica aerogels with various surface-modification agent mixtures (A) HMDSO + HMDZ, (B) TMCS + HMDZ, and (C) TMCS + HMDSO

at the final stage of drying due to tiny pores causes a further compacting structure and leads to nanoporous structure of 5 nm pore size distribution, whereas in the case of aerogel C, due to absence of OH end group condensation in the gels, there is remarkable change in the structure due to inhibition of shrinkage, resulting in the nanoporous structure, high pore volume with low dense aerogels with uniform pore size distribution of 11 nm.

Transmission electron microscopy

Microstructure and particle morphology of the aerogels obtained by TEM for various CSMAs have been shown in Fig. 11a–c. The aerogel A has a highly dense surface morphology and compact structure as shown in Fig. 11a. A uniform and nanoporous, well-structured network was observed in the aerogel C mixture of Fig. 11c which resulted by complete surface modification, hence free from capillary pressure during drying. The structure of the aerogel B was cluster formation with big pores due to the effect of ammonium chloride as shown in Fig. 11b and are opaque as shown in Fig. 1b. The porous network of the aerogel B is due to some what better surface modification than the A because of TMCS in the B.

TGA-DTA

The aerogels of the various CSMAs underwent thermal analysis by TGA-DTA method for the stability of hydrophobicity against temperature in the range of room to 600 °C as shown in Fig. 12. It was observed that there was not much change in the structure of the aerogels with increase of temperature to 400 °C except the expulsion of water molecules if present in the materials, but there is sudden decrease in the weight and a peak in the DTA was observed around the temperature 425 °C, which resulted due to the dissociation of the surface organic groups that are unstable at that temperature leaving the aerogels to turn into hydrophilic. The intensity of the peaks was less in the aerogel A and more for the aerogel C as shown in Fig. 12 as it is already mentioned that the surface modification with Si–CH$_3$ groups is less in the aerogel A than the aerogel C. Finally it can be said that the aerogels C can be used as a hydrophobic materials up to the temperature of 425 °C.

Effect of humid atmosphere

To know the retainability of hydrophobicity in the aerogels with time, various CSMAs have been tested in the humid atmosphere for a period more than 12 months by keeping
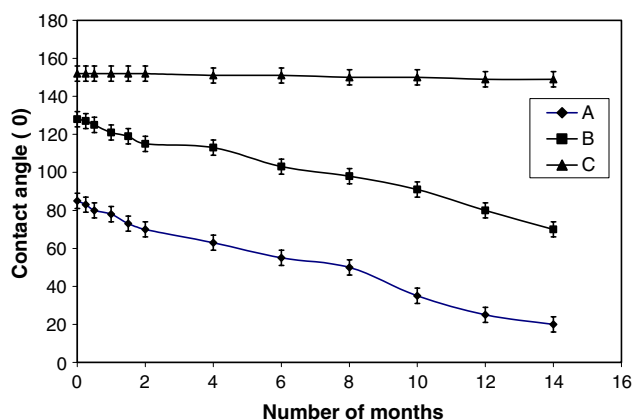
Fig. 12 DTA-TGA of the aerogels for various surface-modification agent mixtures (A) HMDSO + HMDZ, (B) TMCS + HMDZ, and (C) TMCS + HMDSO

**Fig. 13** Change in the contact angle of the aerogels with time in the humid atmosphere for various surface-modification agent mixtures (*A*) HMDSO + HMDZ, (*B*) TMCS + HMDZ, and (*C*) TMCS + HMDSO

the aerogels in the humid surrounding and measuring the contact angle at definite intervals of time as shown in Fig. 13. It was observed that there is negligible decrease in the contact angles of the aerogel C mixture even after 12 months and whereas there is a sudden drop in the contact angle in the aerogels of A mixture due to insufficient surface modification, the aerogels absorbed the water and hence they are unstable in the humid atmosphere. It can be said that the aerogels C can be used for the thermal insulation materials even at temperature of around 400 °C and humid atmospheres for more than 12 months.

## Conclusions

Silica aerogels were prepared with the various combinations of surface-modification agents of HMDSO + HMDZ (A), TMCS + HMDZ (B), and TMCS + HMDSO (C), and the effect of these mixtures on the surface energies, hydrophobicity, contact angle of the aerogels, and related physical properties were studied. It was found that there is a great improvement in the properties of the aerogels with respect to hydrophobic nature with the combination of HMDSO and TMCS surface-modification agents. The surface energy is low (3.39 N/cm), the hydrophobicity is very high (154° conctangle), low dense (0.042 g/cc), and low thermal conductive (0.050 W/km) and less adhesive to water were resulted with the use of TMCS and HMDSO for surface modification. It was found from the TG-DTA of the aerogels that the hydrophobicity in the aerogels remained up to the temperature of 425 °C and above which the aerogels become hydrophilic. The TMCS + HMDSO aerogels were hydrophobic for a period of more than 1 year in the ambient atmosphere.

## References

1. Yoldas BE, Annen MJ, Bostaph J (2000) Chem Mater 12:2475
2. Forest L, Gibiat C, Woignier T (1998) In: Proceedings of the fifth international symposium on aerogels (ISA 5). J Non-Cryst Solids 225:287
3. Guise MT, Hosticka B, Earp BC, Norris PM (1995) In: Proceedings of the fourth international symposium on aerogels (ISA 4). J Non-Cryst Solids 186:317
4. Pajonk GM (1991) Appl Catal 72:217
5. Venkateswara Rao A, Hegde ND, Hirashima H (2007) J Colloid Interface Sci 305:124
6. Kim GS, Hyun SH (2004) Thin Solid Films 460(1–2):190–200
7. Jones SM (2007) J Sol-Gel Sci Technol 40(16):351
8. Kistler SS (1931) Nature 227:741
9. Nakajima K et al (1996) Kogyo-zairyo 44:68
10. Brinker CJ, Scherer GW (1989) Sol-gel science. Academic, New York
11. Kim GS, Hyun SH, Park HH (2001) J Am Ceram Soc 84:453
12. Deshpande R, Smith D, Brinker CJ (1996) US Patent 5,565,142
13. Parvathy Rao A, Pajonk GM, Venkateswara Rao A (2005) J Mater Sci 40:3481. doi:10.1007/s10853-005-2853-3
14. Parvathy Rao A, Venkateswara Rao A, Pajonk GM, Shewale P (2007) J Mater Sci 42:8418. doi:10.1007/s10853-007-1788-2
15. Parvathy Rao A, Venkateswara Rao A, Gurav JL (2008) J Porous Mater 15:507
16. Shewale P, Venkateswara Rao A, Gurav JL, Parvathy Rao A (2009) J Porous Mater 16(1):101
17. Parvathy Rao A, Venkateswara Rao A (2008) J Non-Cryst Solids 354:10
18. Parvathy Rao A, Venkateswara Rao A, Bangi Uzma K (2008) J Sol-Gel Sci Technol 47:85
19. Shewale P, Venkateswara Rao A, Parvathy Rao A (2009) J Sol-Gel Sci Technol 49:285
20. Uzma K, Bangi H, Venkateswara Rao , A Parvathy Rao (2008) Science and Technology of Advanced Materials 9
21. Chibowski E (2003) Adv Colloidal Interface Sci 103:149
22. van Oss CJ, Giese RF, Wu W (1998) J Dispers Sci Technol 19:1221
23. Blake TD (1993) In: Berg JC (ed) Wettabiltiy. Marcel Dekker, New York
24. Cassie ABD, Baxter S (1944) Trand Faraday Soc 43:546
25. Wenzel RN (1936) Ind Eng Chem 28:988
26. Dettre RH, Johnson RE Jr (1963) Adv Chem Soc 43:136
27. Drelich J, Miller JD, Good RJ (1996) J Colloid Interface Sci 179:37
28. Drelich J (1997) J Adhes 63:31
29. Tien P, Chau LK (1999) Chem Mater 11:2141
30. Lee CJ, Kim GS, Hurd AJ (2002) J Mater Sci 37(11):2237. doi:10.1023/A:1015309014546
31. Prakash SS, Brinker CJ, Hurd AJ (1995) J Non Cryst Solids 190(3):264
32. Jeong AeY, Goo SM, Kim DP (2000) J Sol-Gel Technol 19:483
33. Shi F, Wang LJ, Liu JX, Li N (2004) Building materials 6:9, in Chinese
34. Fidalgo A, Ilharco LM (2005) Microporous Mesoporous Mater 84:229
35. Rouquerol F, Rouquerol J, Sing K (1999) Adsorption by powders and porous solids, principles, methodology and applications. Academic Press
36. Barret EP, Joyer LG, Halenda PP (1951) J Am Chem Soc 73:373